Vehicle Description Form

Human Powered Vehicle Challenge 2013

(Form 6)

Latin America: Univ Simon Bolivar, Caracas, Venezuela Feb 22-24
West: NASA Ames Research Ctr, Moffett Field, CA April 12-14
East: Ferris State University, Big Rapids, MI April 26-28

http://go.asme.org/HPVC

This required document for all teams is to be incorporated in to your Design Report. Please Observe Your Due Dates **Latin America Feb 1** **WEST March 11** **EAST March 25**

Vehicle Description

Competition Location: Big Rapids, MI
School name: Rose-Hulman Institute of Technology
Vehicle name: Celeritas
Vehicle number 01

Vehicle type Unrestricted x Speed_____

Vehicle configuration

Upright _____ Semi-recumbent x
Prone _____ Other (specify) _____

Frame material Carbon Fiber, Steel
Fairing material(s) Carbon, Kevlar, Nomex
Number of wheels 2
Vehicle Dimensions *(please use inches, pounds)*

Length 95.00 in Width 18.45 in
Height 41.51 in Wheelbase 43.24 in

Weight Distribution Front 55% Rear 45% Total 100%
Wheel Size Front 16 in Rear 16 in
Frontal area 547.2 in^2
Steering Front x Rear _____
Braking Front _____ Rear _____ Both x
Estimated Cd 0.69

Vehicle history (e.g., has it competed before? where? when?) Celeritas was designed, tested, and constructed in the 2012-2013 competition season by the Rose-Hulman Institute of Technology Human Powered Vehicle Team. This vehicle has not yet competed in competition.

Rose-Hulman Institute of Technology

2013 ASME East Coast HPV Challenge

Presents

Celeritas

Team Officers

Drew Robertson
Patrick Woolfenden
Harrison Coons
Simon Burns
Matt Skorina

Team Members

Jeff Dovalovsky
Ben Griffith
Crystal Hurtle
Garrett Meyer
Melissa Murray
Claire Stark
Clay Dolesh

Travis Tatlock
Louis Vaught
Patrick Woolfenden
Elena Chong
Homa Hariri
Luke Brokl
Jake Hiday

For more team information visit the team website at:
hpvt.rose-hulman.edu

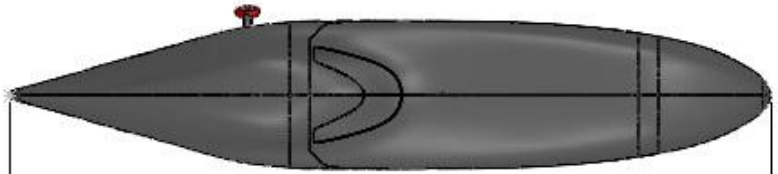

OVERALL LENGTH
95.00in
[2413mm]

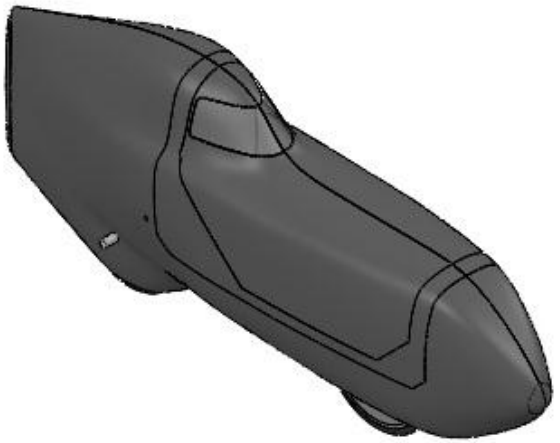

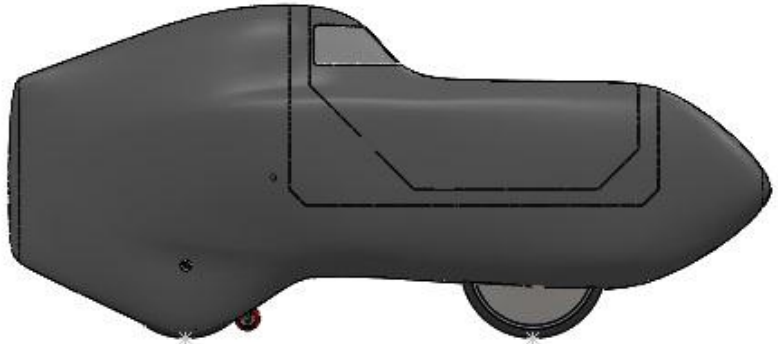

WHEELBASE
43.24in
[1098.32mm]

OVERALL
HEIGHT
41.51in
[1054.31mm]

OVERALL WIDTH
18.45in
[468.63mm]

Abstract

During the 2012-2013 competition season, the Rose-Hulman Human Powered Vehicle Team designed and constructed Celeritas—a lightweight, efficient, and agile human-powered vehicle that can safely and effectively be used for everyday transportation. The project's scope included all aspects of vehicle design and fabrication. The team conducted analysis, computational modeling, and physical testing to demonstrate that Celeritas met the safety and feature requirements of Rose-Hulman Institute of Technology, Human Powered Race America events, and the ASME Human Powered Vehicle Challenge.

Within these requirements, the team designed Celeritas with the objectives of exceptional performance, practicality, and safety. The vehicle is a semi-recumbent bicycle with a carbon fiber structural fairing. The fairing weighs 25 lb_f (111 N) and was the product of a six-piece mold, which eliminated seaming. This design strengthened the fairing and removed 7 lb_f (31.2 N) of weight.

The choice of standard bicycle components and sub-frame made of rectangular 4130 steel tubing increased reparability and durability. The team designed Celeritas to have high stability at expected riding speeds, an innovative and robust electronic landing gear, and an internally geared hub (which allows shifting while stopped) to create easy, unassisted stops and starts. These features combine with a grocery bag-sized storage space and a hazard flag to make Celeritas a highly practical vehicle.

The team held rider safety paramount in the design of Celeritas. The vehicle boasts a forward field of vision of 200 degrees and a protective layer of Kevlar to guard against penetrating debris. Both its three-point safety harness and maximum top load on the roll bar tested at twice ASME specifications. The team also introduced an innovative anti-lock braking system to guard against loss of rider control. With robust and novel engineering, Celeritas advances the field of human-powered vehicles.

1 Design

1.1 Objective

The Rose-Hulman Human Powered Vehicle Team designed, analyzed, and constructed Celeritas during the 2012-2013 competition season guided by the team's mission statement:

> The Rose-Hulman Human Powered Vehicle Team has the goals of furthering the field of human-powered vehicles, creating a common library of knowledge pertaining to their design and construction, developing innovative processes and designs, and providing a positive learning and working environment for students.

The team designed Celeritas with the goal of creating a lightweight, efficient, and agile human-powered vehicle that can safely and effectively be used for everyday transportation.

1.2 Background

Rising energy costs and increasing greenhouse gas levels have led companies and governments worldwide to invest in sustainable and reliable forms of energy and transportation. In the past 10 years an increasing number of people have turned to bicycles for everyday transportation and short trips around town [1]. Bicycles are an economic and efficient mode of transportation with no fossil fuel consumption. Unfortunately, the unfaired upright bicycle has a low top speed and offers little storage space and safety features compared to the average automobile.

The team sought to create a vehicle that surpasses the efficiency of an unfaired upright with the convenience and safety of an automobile. Moving the rider to a recumbent position and adding an aerodynamic fairing to the design allows for greater speed over longer distances while also protecting the rider from their surroundings. A storage space behind the rider allows for further practicality. With its increased efficiency, rider protection, and storage space, the faired recumbent represents a niche in the sustainable transportation market that has not yet been capitalized.

1.3 Prior Work

Over the past several years, the team has gained experience in the design and construction of fared recumbent vehicles. Each year the team draws on past experience to improve the design and create new and innovative features.

A small frontal area for Celeritas was obtained with the help of two design features from the 2009 Mark IV: a pass-through rear axle, and a narrow Q-factor (pedal to pedal width) [2].

From the 2010 Ragnarök, Celeritas incorporated an ergonomic seat and a flip-up tiller for ease of ingress and egress. Wind condition analysis procedures developed for the 2010 Ragnarök were also re-used to determine what crosswinds the vehicle should be designed to handle [3].

Celeritas was designed to closely fit riders with the help of a 3-D motion capture processing program initially developed for the 2011 Helios [4].

Many aspects of the 2012 Carŋot were also utilized in the design of Celeritas. The telescoping landing gear system was improved with an innovative electronic actuation design. Celeritas incorporates a redesigned structural fairing which retains the ribbed tub concept of the Carŋot but offers improved clearances between the rider and the fairing. The team duplicated the success of the snap fit hatches on Celeritas. Stability was analyzed using a MATLAB program developed for the Carŋot. Improved placement of automotive trim, originally used on the Carŋot, provides superior protection against skidding and wear. Similar to the Carŋot's safety features, Celeritas uses an integrated composite roll bar, which has been redesigned to allow improved seat placement, and a lighter, more effective interior layer to protect riders if the fairing is damaged [5].

1.4 Design Specifications

The team created a list of goals and constraints for Celeritas based on rules for the ASME Human Powered Vehicle Competition (HPVC), Human Powered Race America (HPRA) events, and restrictions imposed by Rose-Hulman.

Table 1: Constraints for Celeritas Design

ASME HPVC	**Rose-Hulman**	**HPRA**
15 ft (4.57 m) minimum turning radius	Total cost of materials and consumables of less than $10,000	Rear-view mirrors
Braking from 15 to 0 mph (24.24 to 0 kph) in less than 20 ft (6.10 m)	Less than 8 ft (2.43 m) in length	Independent and redundant braking system
Cargo area able to hold a reusable grocery bag of dimensions: 15 x 13 x 8 in (38 x 33 x 20 cm)	No exposed carbon fiber near rider	
Rider safety harness	Paint the vehicle with traditional school colors (red, white, and black)	
Roll bar that can support 600 lb_f (2.67 kN) top load with elastic deflection less than 2 in (5.1 cm) and 300 lb_f (1.33kN) side load with elastic deflection less than 1.5 in (3.8cm)		

1.5 Concept Development & Selection Methods

The team used a House of Quality (HoQ) to balance the design considerations for Celeritas. The HoQ shows needs ranked 1-5 as rows and metrics as columns. Improvement ratios (shown on the far right) of greater than one indicate on which categories the team focused its efforts. The correlation values between needs and metrics, relative importance values, and extent of influence were assigned by team consensus.

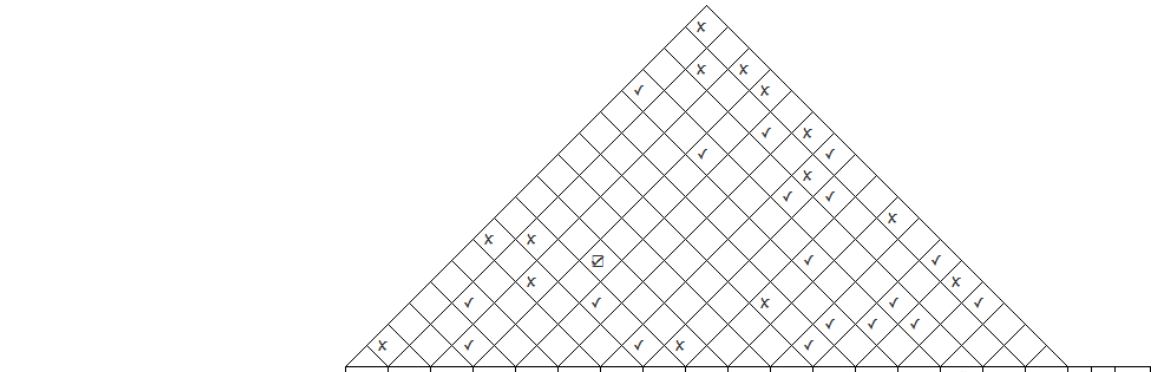

		Roll Bar Strength	Field of View	Turning Radius	Rider Satisfaction with Handling	Percent of Max. Power Produceable	Drivetrain Efficiency	Weight	Cd*A	# of Falls per 10 Stops & Starts	Innovation Score	Construction Time	Number of Parts	Max. Tolerances for Functional Vehicle	Mean Time Between Failures	Longest Non-Catastrophic Repair Time	Vehicle Volume	Cost	Current Competition	Planned Product	Improvement Ratio
minimizes rider injury	5	9	1	1	1					3									4	5	1.25
allows riders to be aware of surroundings	5		9																4	4	1.00
handles well	5			9	9					3									3	4	1.33
allows riders to effectively propel vehicle	4					9	9	1	3										4	4	1.00
accelerates quickly	4					9	9	9	9										3	4	1.33
has low wind resistance	4								9										4	4	1.00
transistions well between stationary and moving	4				3					9									3	5	1.67
tolerates all road and weather conditions	4								3						3				4	4	1.00
is innovative	4										9								3	4	1.33
has manageable construction	4											9	9	9				1	3	3	1.00
is durable	4	3								3			3	3	9				4	4	1.00
is quickly repairable	3												9	3		9		1	4	4	1.00
is easily repairable	3													3	1	9			4	4	1.00
is easily transportable	3							9									9		3	4	1.33
is low cost	2												1					9	3	4	1.33
Absolute Importance		57	50	50	62	72	72	67	96	78	36	36	77	66	51	54	27	25	976		
Relative Importance		9	12	12	8	4	4	6	1	2	14	14	3	7	11	10	16	17			
Current Performance		1200	270	25	7	30	90	75	0.31	1	19.2	2200	100	2	2	90	20.7	2150			
Improvement Direction		▲	▲	▼	▲	▲	▲	▼	▼	▼	▲	▼	▼	▲	▲	▼	▼	▼			
Target Performance		1220	300	20	8	40	94	60	0.25	0	26	2000	80	4	50	45	17	1900			
Units		lbs	deg	ft	1-10	%	%	lbs	ft^2	falls		hrs	parts	%	hrs	min	ft^3	$			

Figure 1: House of Quality for Celeritas Design

Based on these HoQ shown in Figure 1 above, areas of focus were determined to be the coefficient of drag times the cross-sectional area, starting-stopping capabilities, acceleration, and innovation. Improving these areas would have to come at the expense of other categories analyzed in the HoQ, but the other categories had lower importance and could stand to stay the same or decrease slightly. For example, improving the aerodynamics of the vehicle would come at the expense of the rider comfort but the HoQ shows that rider comfort is of lower importance.

1.6 Organizational Timeline

The Gantt chart in Figure 2 was used to make sure that the team could successfully complete a vehicle meeting all of the design constraints and objectives within one academic year. The beginning of the year was dedicated to designing Celeritas and introducing new members to the team, while the second half of the year was spent constructing Celeritas and documenting work.

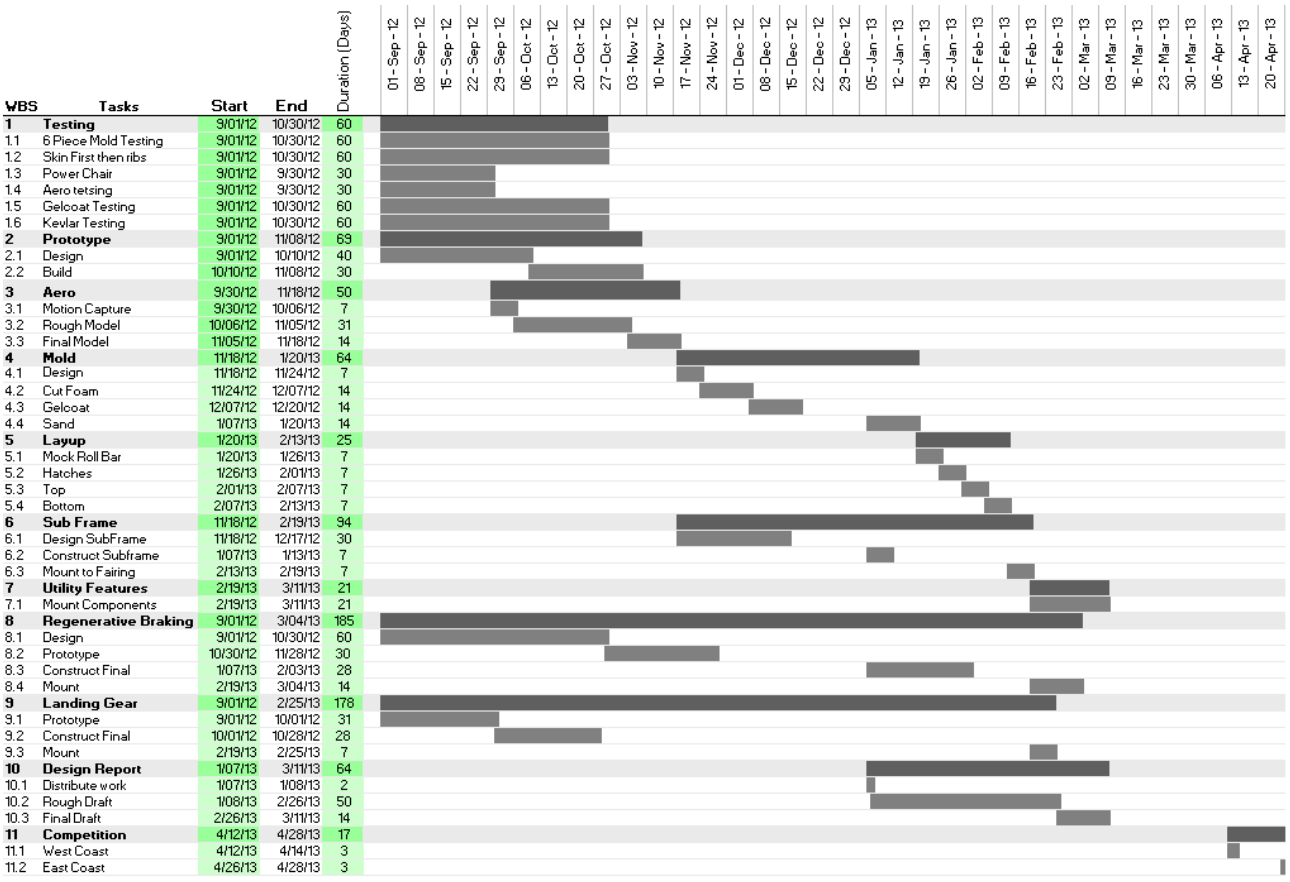

WBS	Tasks	Start	End	Duration (Days)
1	**Testing**	9/01/12	10/30/12	60
1.1	6 Piece Mold Testing	9/01/12	10/30/12	60
1.2	Skin First then ribs	9/01/12	10/30/12	60
1.3	Power Chair	9/01/12	9/30/12	30
1.4	Aero tetsing	9/01/12	9/30/12	30
1.5	Gelcoat Testing	9/01/12	10/30/12	60
1.6	Kevlar Testing	9/01/12	10/30/12	60
2	**Prototype**	9/01/12	11/08/12	69
2.1	Design	9/01/12	10/10/12	40
2.2	Build	10/10/12	11/08/12	30
3	**Aero**	9/30/12	11/18/12	50
3.1	Motion Capture	9/30/12	10/06/12	7
3.2	Rough Model	10/06/12	11/05/12	31
3.3	Final Model	11/05/12	11/18/12	14
4	**Mold**	11/18/12	1/20/13	64
4.1	Design	11/18/12	11/24/12	7
4.2	Cut Foam	11/24/12	12/07/12	14
4.3	Gelcoat	12/07/12	12/20/12	14
4.4	Sand	1/07/13	1/20/13	14
5	**Layup**	1/20/13	2/13/13	25
5.1	Mock Roll Bar	1/20/13	1/26/13	7
5.2	Hatches	1/26/13	2/01/13	7
5.3	Top	2/01/13	2/07/13	7
5.4	Bottom	2/07/13	2/13/13	7
6	**Sub Frame**	11/18/12	2/19/13	94
6.1	Design SubFrame	11/18/12	12/17/12	30
6.2	Construct Subframe	1/07/13	1/13/13	7
6.3	Mount to Fairing	2/13/13	2/19/13	7
7	**Utility Features**	2/19/13	3/11/13	21
7.1	Mount Components	2/19/13	3/11/13	21
8	**Regenerative Braking**	9/01/12	3/04/13	185
8.1	Design	9/01/12	10/30/12	60
8.2	Prototype	10/30/12	11/28/12	30
8.3	Construct Final	1/07/13	2/03/13	28
8.4	Mount	2/19/13	3/04/13	14
9	**Landing Gear**	9/01/12	2/25/13	178
9.1	Prototype	9/01/12	10/01/12	31
9.2	Construct Final	10/01/12	10/28/12	28
9.3	Mount	2/19/13	2/25/13	7
10	**Design Report**	1/07/13	3/11/13	64
10.1	Distribute work	1/07/13	1/08/13	2
10.2	Rough Draft	1/08/13	2/26/13	50
10.3	Final Draft	2/26/13	3/11/13	14
11	**Competition**	4/12/13	4/28/13	17
11.1	West Coast	4/12/13	4/14/13	3
11.2	East Coast	4/26/13	4/28/13	3

Figure 2: Gantt Chart Scheduling the 2012-2013 Competition Season

1.7 Innovation

Following the mission statement, the team strives to create innovative solutions to problems common to recumbent vehicles. For the 2012-2013 competition year, the team decided to focus on preventing the brakes from locking, improving the landing gear system, and removing seams from the final vehicle using a six-piece mold.

1.7.1 Anti-Lock Braking System

Due to the weight distribution in previous years' vehicles, riders required significant experience to avoid locking up the rear wheel while braking. The team rectified this through an anti-lock braking system (ABS), similar to those used in automobiles. The ABS lowers the skill required for operation of Celeritas and improves handling in adverse conditions, thus enhancing the safety of the vehicle.

The ABS continually monitors the rotation of the rear wheel using an optical sensor to watch for black strips painted on the rim of the wheel. When the rider pulls the rear brake lever, a sensor detects how far the brake lever was depressed and a microcontroller relays a proportional signal to a servo motor which actuates the rear disc brake. If at any time the optical sensor detects wheel lock, the microcontroller reduces the braking force until the wheel turns.

Further details on the ABS can be found in Appendix One.

1.7.2 Landing Gear Drive Mechanism

The landing gear system allows the rider to stop and start during the endurance race without removing the canopy. To maintain the vehicle's aerodynamic integrity the landing gear retracts into the fairing similar to an airplane's landing gear. In the 2012 Carŋot Cycle, the actuation mechanism for the landing gear was a manual pull cable which was prone to locking up and disengaging without user input. To alleviate this problem in Celeritas, the team decided to pursue an electric drive to control the actuation and retraction of the landing gear. This system increases ease of use and reduces the possibility of user error.

Previous teams have pioneered electronically actuated landing gear; Celeritas uses an innovative electronic design which is simpler and more robust. Celeritas replaces semiconductor devices, sensors, and signal conditioning circuitry with a set of three mechanical switches. A schematic for the landing gear circuit can be found in Figure 3.

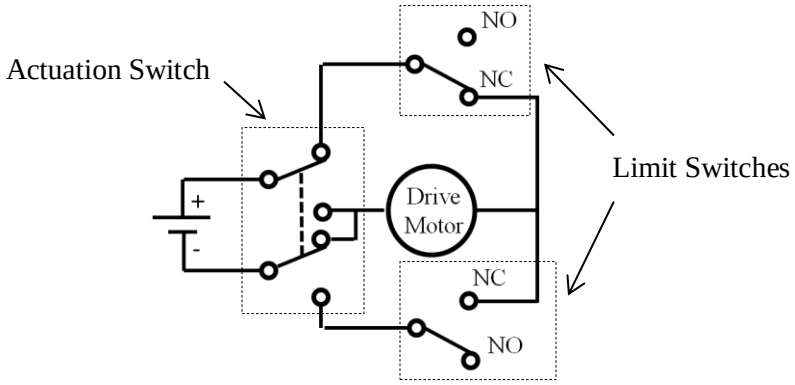

Figure 3: Landing Gear Electronics Schematic (NC=Normally Closed, NO=Normally Open)

An actuation switch selects which direction the motor should turn. Once the landing gear has fully deployed or retracted, one of the two limit switches will cut power to the motor depending on its direction. This simple design is extremely efficient, reduces part costs and assembly time, and is less vulnerable to damage by moisture or impact loading.

1.7.3 Six-Piece Mold

The team has traditionally made large composite parts in two halves and then seamed them together. This often resulted in misaligned ribs, and ribs could not be placed along the centerline of the vehicle. Seaming the halves of the 2012 Carŋot Cycle took six days of fabrication and added a considerable amount of weight through extra carbon and epoxy. The seams were also weak points prone to fatigue.

The team observed that epoxy does not wick through carbon fiber. This property allows one section of a carbon fiber sheet to be cured during a layup and leave another section of the same sheet uncured. Because dry carbon is left attached to the cured carbon, it can be used in later processes to seamlessly lay up other parts of the vehicle.

In order to take advantage of this, the team required a mold that could be reconfigured. A six-piece mold was used so that the top of the fairing could be laid up while leaving the bottom of

the fairing dry. The mold could then be reconfigured so that the bottom of the fairing could be fabricated to produce a seamless vehicle. This process furthers the field of human powered vehicles by providing a cost-effective solution to producing a seamless fairing with continuous bottom ribs.

For further description on the development and functionality of the six-piece mold, see Section 1.12.

1.8 Frame Design

The Celeritas frame design is based on the same fundamental design as the 2012 Carŋot Cycle. The frame is a ribbed tub monocoque and a sub-frame to mount the front wheel and pedals.

Ribs consisting of unidirectional carbon fiber around a Nomex core bear the majority of the load in the fairing. The monocoque fairing design allows the team to use the aerodynamic skin as a supplemental support structure. The carbon fiber ribs are positioned as shown in Figure 4 to provide the optimal weight distribution. The use of composites results in a lightweight and durable fairing.

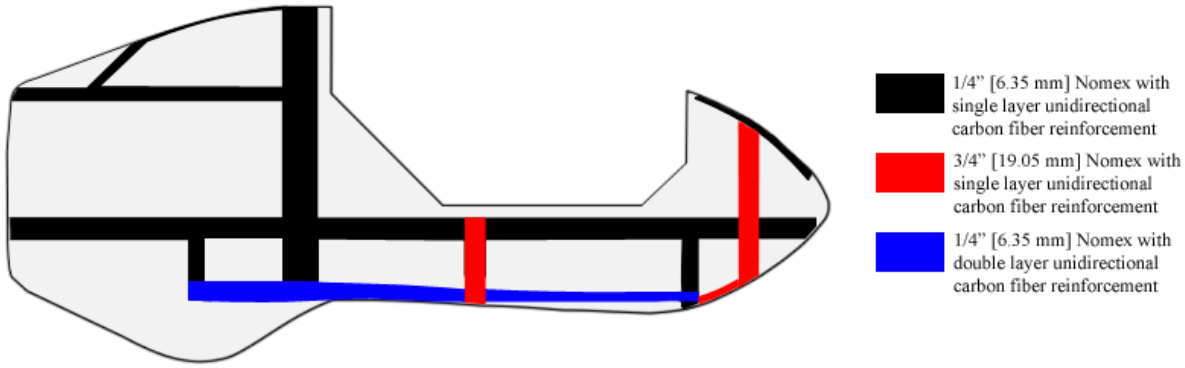

Figure 4: Nomex Rib Layout

The Celeritas frame differs from the 2012 Carŋot Cycle in its use of a steel sub-frame, described in Section 2.2, and ribs placed in the middle of vehicle. One of the benefits of the six-piece mold is the ability to put supporting ribs in the middle of the vehicle, where they provide strength without interfering with the rider. Previous manufacturing methods precluded placing ribs along the centerline of the vehicle due to seaming requirements.

1.9 Roll Bar

An integrated composite roll bar protects the rider. Although conceptually similar to previous years, a new design was created to allow optimal seat placement. The roll bar's cross-member, which helps support side loads, is 6 in (15.2 cm) lower than in last year's design to better brace the seat. To meet the stiffness requirements with this geometry, additional unidirectional carbon fiber was used as compared to previous designs. Using less carbon fiber weave keeps the overall weight the same, and partially offsets the cost of the additional unidirectional carbon fiber. The layup schedule from inside to outside is shown in Figure 5.

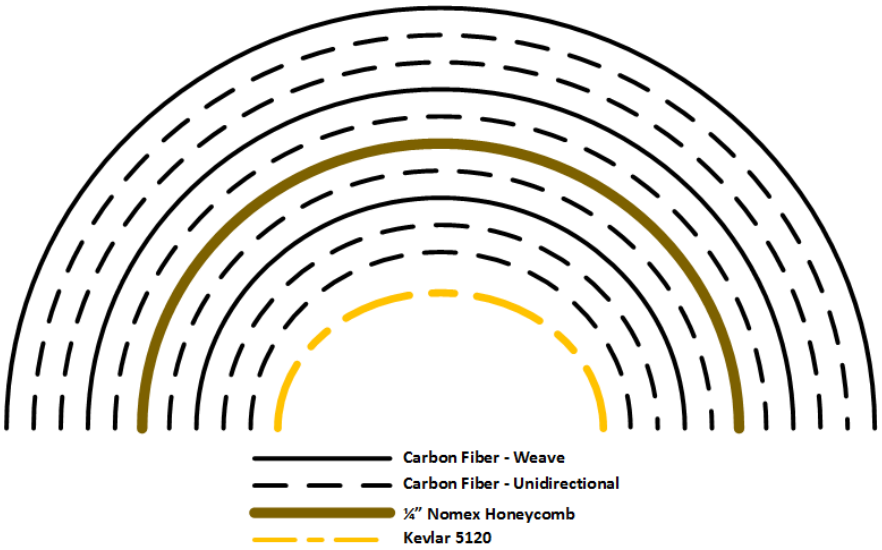

Figure 5: Roll Bar Components

1.10 Landing Gear

The landing gear consists of a slider, a drive mechanism, and a locking mechanism. The landing gear system is located behind the rider, on the left side of the vehicle. A rendering of the landing gear is shown in its retracted position in Figure 6.

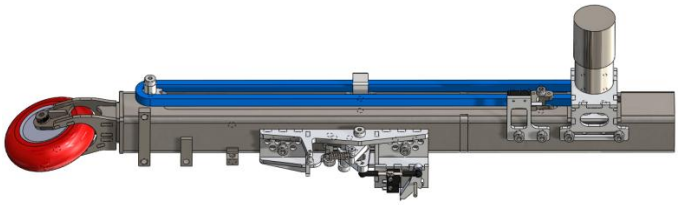

Figure 6: Landing Gear in Retracted Position

1.10.1 Slider

The slider is comprised of two telescoping steel tubes. The tubes do not slide directly against each other as in the 2012 Carɳot Cycle, but rather use a machined Delrin rail to align the tubes as shown in Figure 7. The Delrin rail minimizes both friction and tolerance stack-up because it is machined to the size necessary to align the tubes. The Delrin rails are fixed between the tubes and end caps.

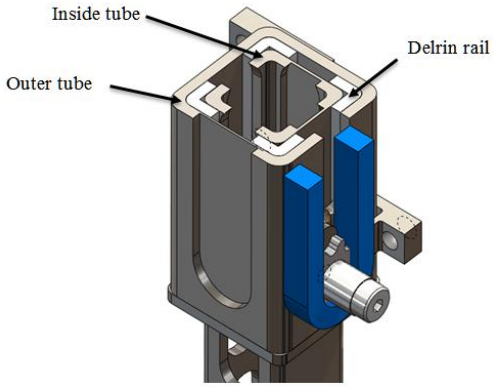

Figure 7: Cross-section of Landing Gear Showing Slider

1.10.2 Locking Mechanism

To prevent the weight of the vehicle from back driving the motor and damaging the drive mechanism, a locking mechanism was designed to mechanically hold the landing gear in its engaged position.

Once the inner tube is extended, a spring pulls the latch into the locked position. Limit switches on the locking mechanism turn the motor off when fully extended. A rendering of the locking mechanism as well as a cross-sectional view showing the latch can be seen in Figure 8.

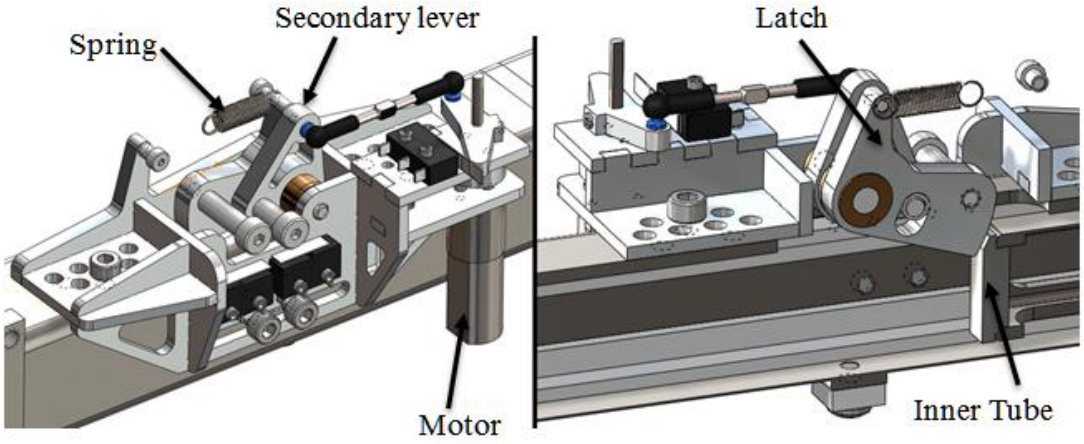

Figure 8: Landing Gear Locking Mechanism

A 12 volt geared motor drives a chain to move the inner tube. The motor's power and gearbox ratio were selected to extend or retract the landing gear in less than 3 seconds with minimal weight. A rendering of the drive mechanism can be found in Figure 9.

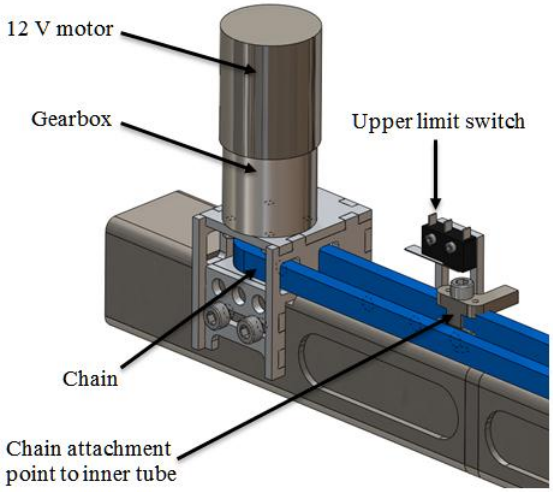

Figure 9: Landing Gear Drive Mechanism

1.11 Drivetrain

For Celeritas, the team desired a more robust drive train with a smaller size than in previous years. The 2012 Carŋot Cycle used a drivetrain with normally spaced pedals which required a

widened and lengthened nose to allow space for pedaling. This increased the size of the vehicle and added weight.

1.11.1 Low Q-Factor

The team decided to narrow the spacing for the front cranks to improve aerodynamics and rider power output [6]. This type of design is commonly known as low Q-factor. The difference in final shape is evident, as shown in Figure 10 comparing Celeritas to the 2012 Carηot Cycle, which had a standard Q-factor crank set and bottom bracket.

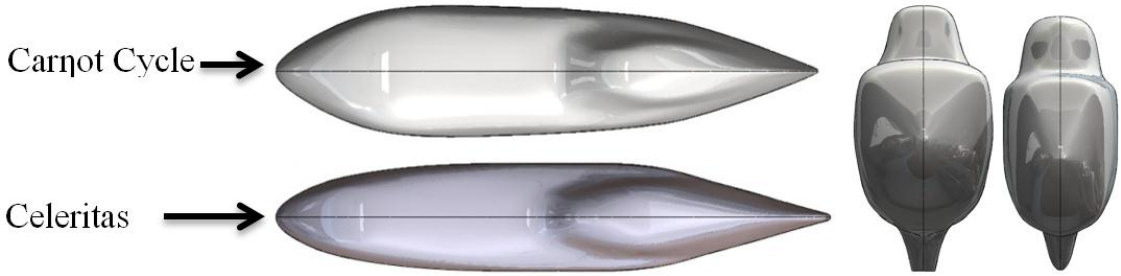

Figure 10: Top (Left) and Front View (Right) Comparison of the 2012 Carηot Cycle and Celeritas

A custom bottom bracket and crank set were manufactured to achieve a lower Q-factor than commercially available options. To align the chain with the crank set and bottom bracket, the team returned to the use of a two-chain drivetrain with a transfer point above the drive wheel.

1.11.2 Internally Geared Hub

The team selected an internally geared hub to improve shifting performance. Because the internally geared hub uses indexed shifting, it is easier for the rider to quickly change gears as well as shift gears while stopped. These advantages are expected to outweigh the lower weight and 3-5% higher efficiency of the traditional cassette system. As a consumer vehicle, this would greatly increase practicality in urban environments where stops are frequent. An internally geared hub keeps the chain line constant which reduces torque steer, resulting in improved handling.

The Celeritas drivetrain also includes a derailleur that both tensions the chain and accommodates a traditional cassette. While the internal hub is preferable, a customer could be flexible in their choice of drivetrain without needing further specialty hardware.

1.12 Rear Hatch Magnetic Attachment

The snap fit grooves on the rear hatch prevent it from moving in any direction but out. Magnets on the rear hatch prevent it from falling by securing it against the fairing. The team drilled eight holes on the inside of the rear hatch in the Nomex ribs and glued in 5/8 in (15.88 mm) neodymium disc magnets, as seen in Figure 11. Eight small matching steel plates were fixed to the inside of the fairing. The combined pull of the magnets approximately equaled 20 pounds, guarding against any unintentional removal.

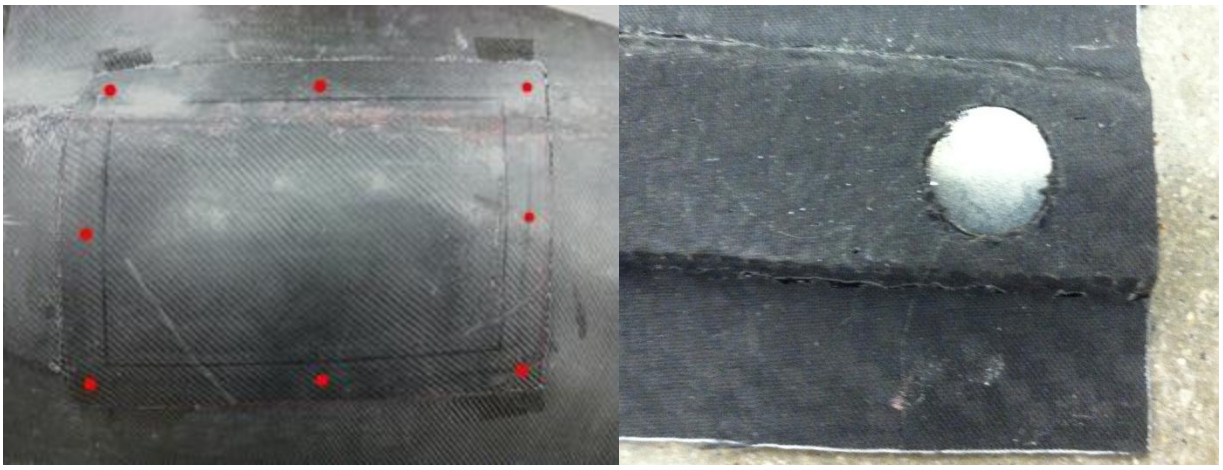

Figure 11: Rear Hatch with Red Dots Marking Magnets (left) and Indented Magnets in a Nomex Rib (right)

1.13 Six-Piece Mold

The team investigated alternative methods to manufacture the fairing to avoid seaming. One required expanding a highly pressurized bladder into the mold cavity. The team's previous molds would be incapable of handling this. Metal molds, which would solve this problem, are not cost effective for one-off production.

In previous years, the team observed that unintended dry spots could occur in the laminate if the reinforcing fibers were not fully impregnated before being placed in the mold, because epoxy cures before it can wick through the fabric. Consequently, applying epoxy to only one area of a reinforcing sheet allows that area to cure in a shape, while the rest of the fabric remains formable. In doing this, a continuous piece of fabric can be laid up in multiple stages.The team laid up Celeritas in two halves using this technique to create a seamless fairing. The routed mold was cut into six pieces to utilize this method.

The first step of this process was to create the hatches that the rider uses to get into the vehicle and access the rear wheel. The top half of the mold was put together and placed in a box to hold them in position. The same configuration was used to lay up the top half of the fairing; epoxy was impregnated into the top half leaving excess carbon for the rest of the vehicle dry.

The lower half of the six-piece mold was placed into the box for the next layup, and the fairing was placed in the mold. The dry carbon from the first layup was then saturated with epoxy. After curing, a full, seamless, monocoque faring was left as shown in Figure 12. The lower half of these six-piece mold was placed into the box for the next layup, and the fairing was placed in the mold. The dry carbon from the first layup was then saturated with epoxy. After curing, a full, seamless, monocoque faring was left as shown in Figure 12.

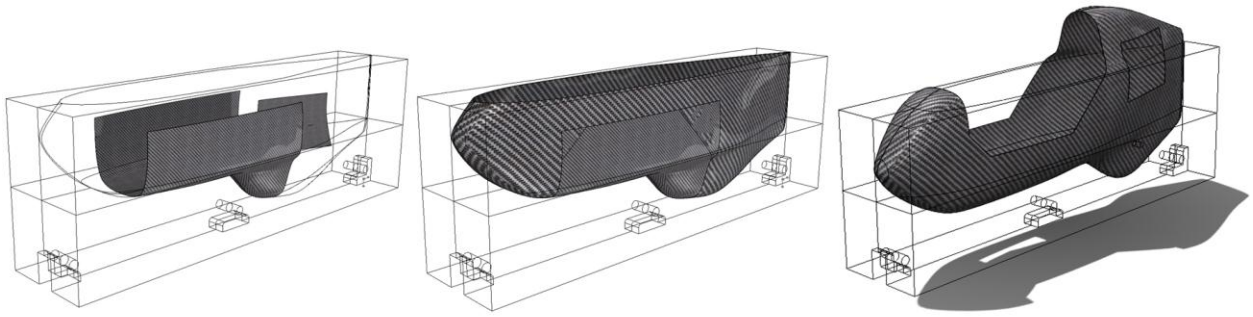

Figure 12: Fairing Layup Steps: Hatches (left), Top Half (middle), and Bottom Half (right)

Using the six-piece mold allowed the team to complete the fairing in only three layups and reduced the weight of the final fairing by 7 lb_f (31.2 N). However, it required more coordination as half the fairing was laid up at a time. The benefit of decreased manufacturing time outweighed the increased difficulty of the layup process.

1.14 Practicality

The use of Celeritas as a practical form of personal transportation guided the decisions of the team. In its construction, standard bicycle components were used where possible for ease of replacement. The composite fairing resists corrosion and can be patched in the event of a puncture. Celeritas has stability at both high and low speeds, and its landing gear system allows it to stop and start unassisted. A storage area also allows for versatility as small items can be transported easily. Celeritas also features a flip up tiller similar to the 2010 Ragnarök. The rider can fold back the hinged steering tiller to make entering and exiting the vehicle easier while still providing adequate tiller length. These features combine to produce a highly practical vehicle.

1.14.1 Fairing Openings

In previous years, the front hatches of the team's vehicles have been small to protect riders from scraping their sides. However, this feature slows ingress and egress and prevents the rider from placing their feet on the ground when inside the vehicle. The team designed the Celeritas front hatch to be larger while still retaining rider safety. Fairing handles, made of 0.75 in (1.9 cm) Nomex, were also placed along the shoulder protection material. These handles allow more area for the rider to support himself. These handles, along with the fairing opening, hasten ingress and egress and allow the rider to be more self-sufficient with the front hatch removed.

The rear hatch opening is designed so that the rear of the vehicle is easily accessible. This allows easy access to the vehicle's storage space, rear wheel, rear disk brake, and landing gear. The rear hatch of 2012 Carnot Cycle sat over the top of the fairing to lend it stability, but the edges did not lay flush to the fairing surface. The Celeritas rear hatch was designed to be one-sided and held on by magnets (see Section 1.12) to rectify this problem.

1.14.2 Storage

The cavity directly behind the rider and above the rear wheel is large enough to contain a reusable grocery bag. The team installed a shelf to support any parcel weighing less than 12

pounds and determined attachment points for bungee cords to secure the bag. The storage space is easily accessible through the rear hatch.

1.14.3 Weather Conditions

Celeritas provides comfort for the rider in a variety of weather conditions. The team determined temperatures from 40°F (4°C) to 95°F (35°C) to be the ideal conditions for riding. According to these criteria, Celeritas is rideable throughout most of the continental United States. The HPVC locations of Big Rapids, Michigan, and Mountain View, California, present two very different weather conditions. According to weather data from The Weather Channel, Celeritas would be rideable from March through November in Big Rapids and throughout the year in Mountain View [7]. This is ignoring average lows which usually occur overnight, when riding is unlikely. According to weather data for Terre Haute, Indiana, the team's headquarters, Celeritas would be rideable approximately 330 days per year.

1.14.4 Communication

The rider needs to interact with the world outside the fairing when entering busy roadways. The turn signals, brake lights, and horn of Celeritas communicate the intentions of the rider, increasing safety. The rider is also provided with a two-way radio and a microphone mounted to the seatbelt for communication with team members while on the track.

2 Analysis

2.1 Rollover Protection System

Table 2: Summary of RPS Analysis

Objective	Method	Results
To prove that the RPS met ASME standards	Hand Calculations were used to determine an estimate of deflection	The roll bar met ASME specification with a top load deflection of 0.63 in (16mm) and a top load deflection of 0.76 in (19 mm)
	ANSYS was used for Finite Element Analysis (FEA) to determine deflection	The roll bar met ASME specification with a top load deflection of 0.32 in (8 mm) and a top load deflection of 1.16 in (29 mm)

The team analyzed the roll bar using basic bending equations and FEA to ensure that the roll bar met the specifications given in Section III.C.1 of the ASME competition rules [8]. The model was simplified by assuming left-right symmetry and an anisotropic material, along with omitting the Nomex rib. The composite's elastic modulus was assumed to be 14 Msi (96.5 GPa), the area-weighted average of unidirectional carbon's longitudinal modulus and carbon weave's modulus.

Hand calculations used beam deflection models to approximate the expected roll bar deflection in top load. For top loading, the load was assumed to be vertical and the cross-member was neglected. The model and results are displayed in Figure 13 and Table 3, respectively.

The side loading was analyzed by treating the sides of the roll bar as a simply supported beam, with the top of the roll bar and the cross-member being treated as columns. The model is displayed in Figure 13. This approximation does not account for the moments applied by the cross member, so the side deflection shown in Table 3 is an overestimate.

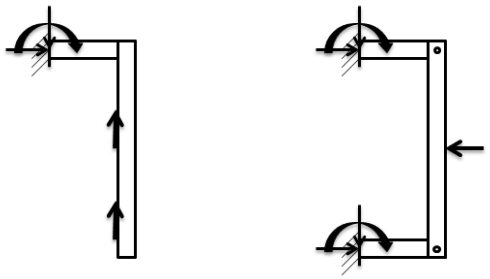

Figure 13: Roll Bar Hand Calculations Models, Top (left) and Side (right)

Analysis of the top and side load was also done in ANSYS to complement the hand calculations. FEA allows for a more accurate model of complex shapes, but the team was limited by available computational power. The ANSYS model assumed that the chrome-molybdenum steel cross-member was perfectly joined to the composite laminate with no mounting hardware.

Static forces were applied to the sides or seatbelt mounts as appropriate, while the top of the roll bar was held fixed. This allowed forces to be applied at seatbelt mounting points which could move as the roll bar deformed, increasing accuracy. ANSYS results are shown in Figure 14, and maximum deflections are summarized in Table 3.

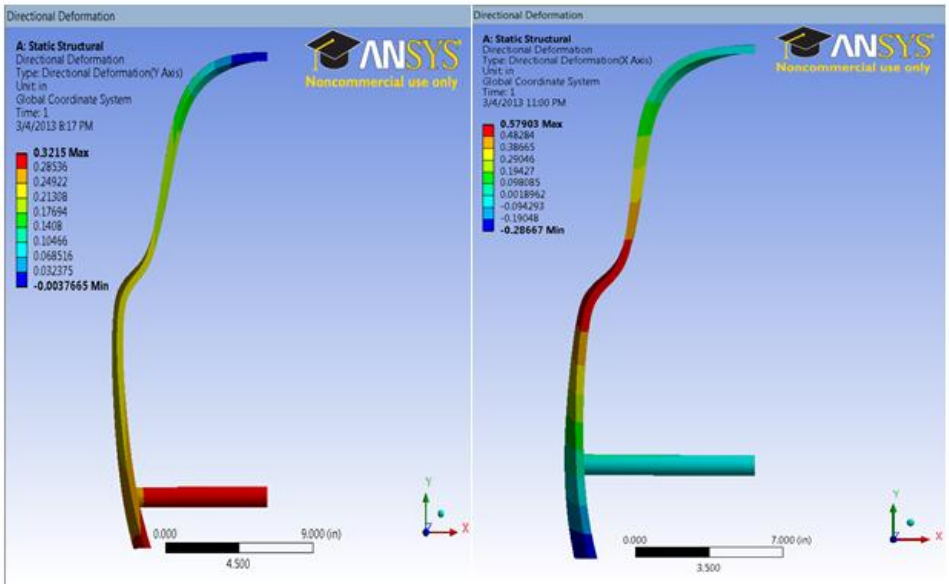

Figure 14: Load Deflections for Roll Bar – Top Load Vertical Displacement (left) and Side Load Horizontal Displacement (right)

Table 3: Summary of Roll Bar Analysis

	Hand Calculation Deflections in (mm)	ANSYS Deflections in (mm)
Top Load	0.63 (16)	0.32 (8.0)
Side Load	0.76 (19)	1.16 (29)

Considering the results of the hand calculations and the FEA, the roll bar design was within the ASME competition specifications.

2.2 Frame FEA

Table 4: Summary of Frame FEA

Objective	Method	Results
Determine whether or not a metal sub-frame could be as light as the 2012 Carŋot Cycle carbon fiber sub-frame	Use FEA to minimize the amount of material necessary to support the loads on the sub-frame	A 4130 steel sub-frame was found to have a weight similar to the reinforced carbon fiber sub-frame of the 2012 Carŋot Cycle

A carbon fiber sub-frame has a better strength-to-weight ratio than steel or aluminum, but requires more steps during manufacturing. Furthermore, the integrated steel plates of the 2012 Carŋot Cycle, that were necessary to prevent the bottom bracket from twisting out of its carbon sub-frame, limited any benefit from carbon fiber's low weight. Steel and aluminum both offer simplified manufacturing processes. Aluminum could yield a lighter sub-frame, but was rejected due to the high difficulty of welding it. Therefore, the leading candidates were a steel sub-frame and the 2012 Carŋot Cycle carbon fiber design. The frame designs were judged on their final weight, manufacturability, ease of mounting into the vehicle, and strength.

The team determined the reaction forces in the bottom bracket using simple kinematic models, as shown in Figure 15.

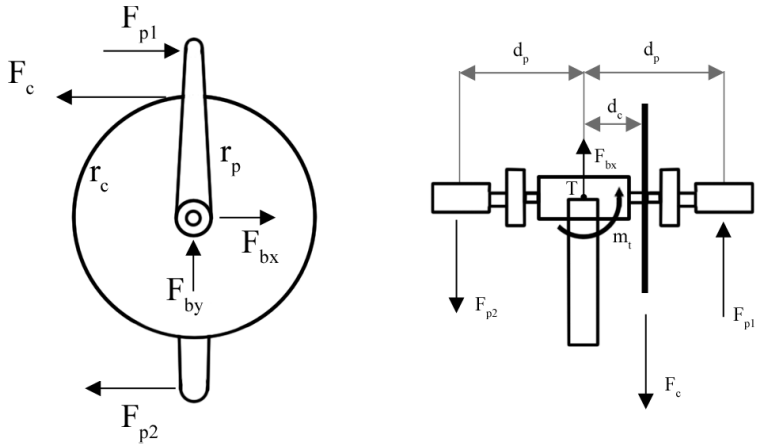

Figure 15: Side (Left) and Top (Right) Views of Forces in the Bottom Bracket

Static analysis based on these models correlated the measurements to the resultant forces and moment described in Table 5.

Table 5: Description of the Variables used in Figure 15

	Name	Description	Measurement
Measurements	F_{p1}	Force on one pedal	100 lb_f (445 N)
	F_{p2}	Force on the second pedal	50 lb_f (222 N)
	r_p	Length of the crank (170 mm)	6.7 in (17 cm)
	r_c	Radius of the chain ring (60 tooth)	4.5 in (11.4 cm)
	d_p	Length from the center of the bottom bracket to the pedal	4.5 in (11.4 cm)
	d_c	Length from the center of the bottom bracket to the chain ring	2 in (5 cm)
Results	m_t	Reaction moment about the center of the bottom bracket	-19 lb_f-ft (-26 N-m)
	F_c	Force in the chain	223 lb_f (992 N)
	F_{bx}	Reaction force in the bottom bracket	173 lb_f (770 N)

Based on beam approximations, 1.5 in (3.81 cm) round bar stock and 1.5 x 1 in (3.81 x 2.54 cm) rectangular tube steel were selected for further analysis. Both models had the same wall thickness and material properties. The team decided to use the rectangular tubing for further analysis because of its higher second moment of inertia and ease of manufacture.

To simulate the rider's pedaling in the model, a moment of 19 lb_f-ft (26 N-m) and a force of 173.33 lbf (771.3 N) were applied to the bottom bracket. A force of 127 lbf (565.2 N) was applied to the head tube to simulate the weight distribution of the rider. After several iterations using these parameters, the team settled on a design that was easy to manufacture and would not yield when subjected to riding conditions. The final ANSYS results are shown in Figure 16.

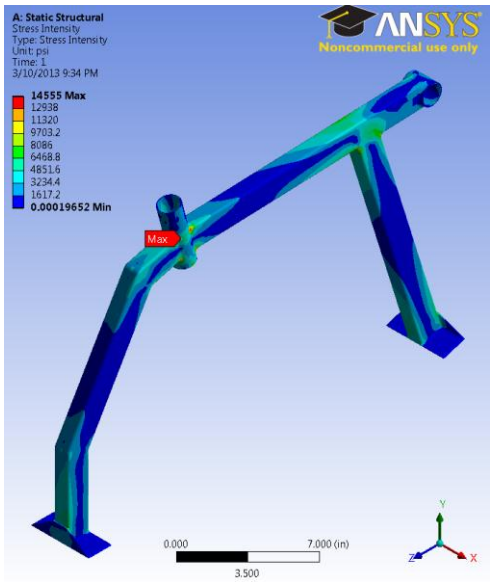

Figure 16: Results of ANSYS Static Loading on Bottom Bracket

The final design of the steel sub-frame used 1.5 x 1 in (3.81 x 2.54 cm) rectangular steel tubing with 0.065 in (2.5 mm) wall thickness. Comparing over a large range of steels, the team selected 4130 steel for the sub-frame because it met the necessary strength requirements with the lowest weight. The design has a factor of safety of 6 and takes into account the effects of impacts.

The final weight of the designed steel sub-frame was 4.8 lb_f (21.36 N) compared to the 5 lb_f (22.24 N) final carbon sub-frame from the 2012 Carŋot Cycle. The steel sub-frame was chosen to replace the carbon sub-frame design in Celeritas because of the similar weights and increased manufacturability.

2.3 Aerodynamic Analysis

Table 6: Summary of Aerodynamic Analysis

Objective	Method	Results
Determine a fairing shape with the least drag force	SolidWorks Flow Simulation was used to determine drag forces	No crosswind drag: 1.43 lb_f (6.36 N). 11.4 mph (18.3 kph) crosswind: 0.57 lb_f (2.54 N)

In order to ensure the fairing would not interfere with the rider's natural pedal stroke, the 3D shape created from the motion capture data was imported into SolidWorks and the fairing design was modeled around it. The team required that each side of the mold could be machined in one single setup; therefore, a maximum width constraint of 18.5 in (46.99 cm) was imposed because of the router dimensions. The team also required a vehicle less than 8 ft (2.44 m) long so that the molds could be routed out of standard size pieces of foam 4 x 8 ft (1.02 x 2.44 m), as well as decrease cost.

A preliminary model was created and iteratively refined in SolidWorks Flow Simulations. The effects of ground and wheel movement were neglected to simplify the computations because their effects were small and did not change significantly when comparing between iterations. Drag forces, streamlines, and the pressure along the surface of the vehicle were viewed after a simulation to determine where improvements could be made. The streamlines around the final fairing are shown in Figure 17.

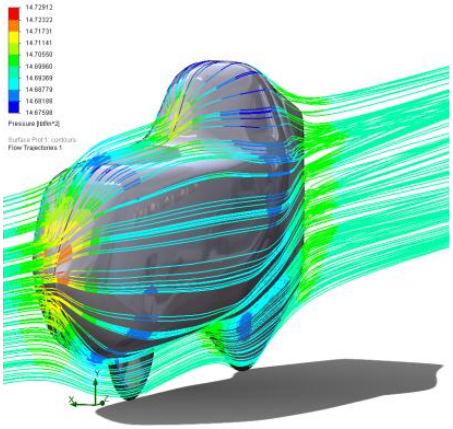

Figure 17: Streamlines at a Vehicle Velocity of 45.5 mph (73.2 kph)

The force results of the flow simulation in comparison to last year's vehicle are shown in Table 7. Celeritas had an 18.2% reduction in drag forces in a no-crosswind situation and a 16% overall reduction in drag forces with an 11.4mph crosswind, which is a considerable improvement over the 2012 Carŋot Cycle.

Table 7: Results from SolidWorks Flow Simulation at a Vehicle Velocity of 45.5 mph (73.2 kph)

	No Crosswind		**11.4 mph (18.3 kph) crosswind**	
	Drag lb_f (N)	**Side Load lb_f (N)**	**Drag lb_f (N)**	**Side Load lb_f (N)**
2012 Carŋot Cycle	1.75 (7.78)	0.00	1.53 (6.81)	16.35 (72.73)
Celeritas	1.43 (6.36)	0.00	0.57 (2.54)	13.88 (61.74)

2.4 Cost analysis

Table 8: Summary of Cost Analysis

Objective	**Method**	**Results**
To determine the cost of producing Celeritas and the cost of a three year production run	Created a financial breakdown of parts, materials, overhead, labor, tooling, and capital investment.	Celeritas, as presented in competition, would cost $2256.51. A production run would cost $6211.15 per vehicle.

The cost associated with producing Celeritas and the cost for a 3 year, 10 vehicles per month production run are summarized in Table 9.

Table 9: Cost Analysis for Celeritas

Category	**Celeritas as presented**	**Production Run (per vehicle)**	**Production Run (360 Vehicles)**
Capital Investment	$0.00	$134.42	$48,390.00
Tooling	$344.82	$344.82	$124,134.84
Parts and Materials	$1,911.70	$1,911.70	$688,210.80
Labor	$0.00	$2,270.00	$817,200.00
Overhead	$0.00	$1,550.22	$558,080.00
Total	$2,256.51	$6,211.15	$2,236,015.28

The estimate for Celeritas includes the costs incurred by the team normalized to one vehicle. The funds for the vehicle were received from the school. Additional funds were received to provide for travel, however, these are not included as they do not affect the vehicle. Capital costs include all machinery and tools used. Labor costs were determined by an estimate for the necessary man-hours to produce vehicles multiplied by an average hourly wage. Approximately 60 hours of labor would be required to manufacture the mold for a Celeritas, which is expected to produce 10 vehicles. The team estimates that 85 man-hours would be required to produce a Celeritas after completion of a mold. It is assumed that a skilled worker would earn $25 per hour. Overhead costs include rent, insurance, and additional staff. The result is $6,211.15 per vehicle.

A detailed analysis of the production run is included as Appendix Two. An analysis for the current vehicle is included as Appendix Three.

2.5 Other Analysis

Additional analyses were performed to examine the speed and handling of the vehicle.

2.5.1 Gearing

Table 10: Summary of Gearing Analysis

Objective	Method	Results
To determine the optimal gearing ratio for Celeritas	A MATLAB program was used to calculate the optimal gearing ratio for Celeritas	Gearing Ratios are shown in Table 11

Gear ranges were selected based on the riders' preferred cadence of 90 rpm and the predominant speed ranges in past races: 15-45 mph (24.1-72.4 kph) for the speed event and 10-35 mph (16-56 kph) for the endurance. By choosing the proper range of gears, Celeritas can achieve these speeds at the optimum rider cadence.

The team used a 60 tooth chain ring and 11-34 tooth cassette as the basis for comparison with the internally geared hub, as discussed in Section 1.11.2. To achieve the desired gear ratios, the optimal input and output sprockets of the mid drive were determined to be 13 and 23 teeth, respectively, and the sprocket on the internally geared hub was determined to be 20 teeth. Listed in Table 11 are the gear ratios and speeds at 90 rpm for each gear of the internal hub and nine-speed cassette.

Table 11: Gear Ratios and Speeds at 90 RPM Cadence

	Internal Hub		**Cassette**	
Vehicle Gear	**Crank to Wheel Ratio**	**Speed at 90 rpm cadence, mph (kph)**	**Crank to Wheel Ratio**	**Speed at 90 rpm cadence, mph (kph)**
1	2.80	13.6 (21.9)	3.12	15.2 (24.5)
2	3.42	16.6 (26.7)	3.54	17.2 (27.7)
3	3.97	19.2 (30.9)	4.08	19.8 (31.9)
4	4.51	21.9 (35.2)	4.62	22.4 (36.0)
5	5.31	25.8 (41.5)	5.31	25.8 (41.5)
6	6.49	31.5 (50.7)	6.24	30.3 (48.8)
7	7.53	36.6 (58.9)	7.08	34.4 (55.4)
8	8.57	41.6 (67.0)	8.17	39.7 (63.9)
9	---	---	9.65	46.9 (75.5)

2.5.2 Stability

Table 12: Summary of Stability Analysis

Objective	Method	Results
Design the vehicle geometry in order to create a stable design	A MATLAB program was used to calculate lowest stable speed	Celeritas is stable at speeds as low as 9.5 ft/s (2.9 m/s)

The optimum rider position and seat angle for Celeritas were experimentally determined using a variable geometry trainer. Given this information, the vehicle's steering geometry was designed using the results of a MATLAB script written by the team. This script uses information from the Lords of the Chainring [9] to calculate the steering geometry of a two-wheeled vehicle. It was used last year with great success on the 2012 Carɳot Cycle. The script calculated the wheelbase and was also used to determine the optimal head tube angle in order to reduce the low speed steering input force, steering sensitivity, and the lowest stable speed of 9.5 ft/s (2.9 m/s).

2.5.3 Turning Radius

Table 13: Summary of Turning Radius Analysis

Objective	Method	Results
To determine the turning radius of Celeritas	Trigonometry was used to determine the final turning radius	Celeritas theoretically has a turning radius of 13 ft (3.96 m)

The turning radius, R, of the vehicle was calculated using the wheel base of the vehicle, L, and the angle of the wheel in a low speed turn, α. The turning radius can be calculated using Equation 4 below.

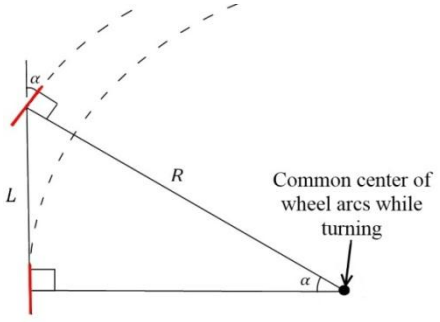

Figure 18: Development of Turning Radius Equation

$$\frac{L}{\sin \alpha} = R \tag{4}$$

Using Celeritas' wheel base of 3.61 ft (1.1 m) and a moderate wheel angle of 16°, the turning radius is calculated to be 13 ft (3.96 m). The result from this analysis was used to design the butterfly-shaped cutout around the front wheel.

3 Testing

3.1 Rollover Protection System Testing

Once the roll bar was designed and analytically determined to meet the rollover protection system specifications listed in the rules, it was necessary to perform physical testing to confirm that it would meet these specifications. To conduct this testing, a duplicate roll bar was created with the same materials and geometry as the one in the vehicle. The specified loads were then applied monotonically using an ATS 1610 UTS tensile tester at the locations described in Section 2.1. The deflections at the specified loads are given in Table 14.

Table 14: Rollover Protection System Analysis and Testing Results

	Hand Calculations, in (cm)	**ANSYS Workbench, in (cm)**		**Physical Testing, in (cm)**
		Axial Deformation	Total Deformation	
Top Load	0.63 (1.6)	0.32 (0.8)	0.50 (1.3)	0.29 (.736)
Side Load	0.76 (1.9)	1.16 (2.9)	1.28 (3.3)	0.28 (.711)

These deformations are below the specified limits. When testing to the specifications, neither visible nor audible indicators of failure were noted, and the resulting force-displacement plots were smooth and reasonably linear, indicating that permanent deformation did not occur. Once the roll bar had supported the specified loads, the roll bar was loaded to failure in the top-loading configuration, supporting a yield load of 1100 lb_f (4.89 kN) and an ultimate load of 1220 lb_f (5.43 kN), for a factor of safety of 1.83.

3.2 Developmental Testing

Testing that contributed to development of key vehicle features are discussed in Sections 3.2.1 to 3.2.8.

3.2.1 Power Output Testing

Multiple variables were tested independently to determine the seat position that gave the highest power output using a variable geometry trainer. Replication was achieved by testing multiple riders. Two characteristics of each trial were recorded. The first characteristic was an average power output reading measured using a power tap hub and recorded using a Garmin cyclocomputer. The second characteristic was a subjective rating of comfort given by the rider after each trial. The geometry variables are described in Figure 19.

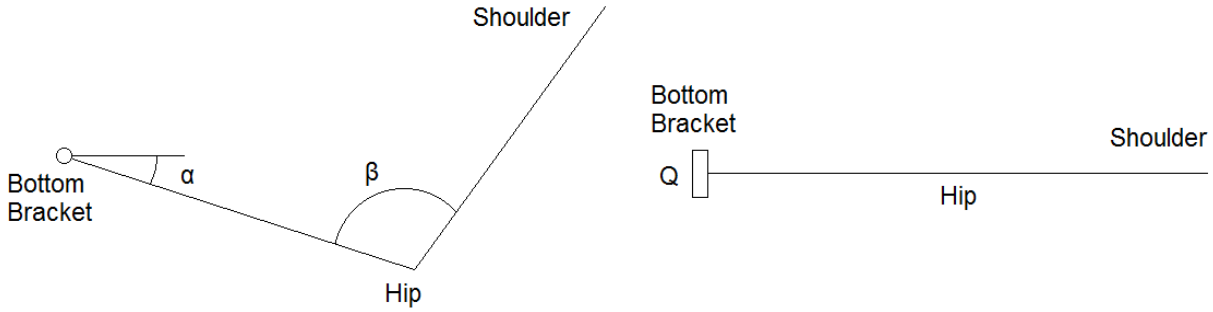

Figure 19: Side and Top Views of the Power Output Testing Geometry

Based on previous experience, riders were allowed to choose comfortable leg extension. The tests began at full speed and consisted of one minute sprints. The team plotted the two criteria against the three variables and found optimal ranges for α and β. A statistical hypothesis test determined that there was no significant correlation between power output and Q-factor. These results are found in Table 15.

Table 15: Results for the Power Output Testing

Variable	Result
α	12-15°
β	120-130°
Q-factor	No Correlation

3.2.2 Motion Capture

The same motion capture procedure developed for the 2011 Helios was used for Celeritas. It produced a model of the volume occupied by the rider of the vehicle. The process was repeated for Celeritas because a new rider position was chosen for the vehicle and low Q-factor cranks were used. Four subjects rode a customizable recumbent trainer for one trial each to obtain a diverse range of rider volumes. To capture all possible motions, the subjects started riding at a slow pace, accelerated, and then sprinted for several seconds. Three Qualisys Track Manager IR cameras were used to capture a model of each rider through the trial. A volume was produced and brought into SolidWorks.

3.2.3 Rib Attachment Method Testing

In previous years, ribs have been laid up on each half of the vehicle along with the skin, after which, the two halves were seamed together. To prevent seaming problems, the team used a six-piece mold, which required the application of certain ribs after the skin cured.

Testing for this project involved creating two laminated samples for a large variety of configurations of carbon fiber and Kevlar. The team's standard practice of rib attachment in previous years has been to lay up the ribs at the same time as the skin which was used as the control. The parameters varied were: carbon fiber or Kevlar; both, one, or neither materials already cured; cured materials sanded or left unfinished; and thick or standard epoxy.

The samples were loaded to failure in a tensile tester. This simulated the shear force endured by the ribs against the skin; the normal force was not tested because it is difficult to replicate.

The team examined the samples where carbon was laid up onto already cured carbon with special interest because it best reflected laying up the ribs after the main fairing had cured. The testing showed that this method was not as effective as epoxying together two layers of already-cured carbon. The samples failed at averages of 2.10 ksi (14.5 MPa) and 2.65 ksi (18.3 MPa) of shear stress, respectively. However, this method was very comparable to the control samples where overlapping carbon pieces were laid up together, which failed at an average of 2.3 ksi (15.9 MPa). This finding helped demonstrate that the team could lay up the ribs after the main fairing cured without unreasonable losses in strength.

3.2.4 Protective Layer Testing

For the past six years, the team has used a layer of Kevlar fabric to protect the rider from debris that could puncture the carbon fiber layer and injure the rider. The team has traditionally used a medium-weight Kevlar 5285 to protect the rider, but alternative protective materials were researched to replace it. Kevlar 5120 was tested against Kevlar 5285 because its lighter weight, 1.8 oz/yd^2 (61 g/m^2) compared to 5.25 oz/yd^2 (178 g/m^2), would reduce the total vehicle weight. Kevlar 5120 also has a much tighter weave than Kevlar 5285 which increases the layer's ability to deflect carbon shards. Two samples each were tested against a control group of bare carbon for protection from carbon shards and pavement abrasion.

The Kevlar samples were laminated onto carbon fiber measuring 6 x 8 in (152 x 203 mm). The samples were tested using a 3-point load until the carbon fiber cracked. Table 16 shows the results of a visual inspection for carbon shards that pierced the protective layer.

The candidate materials also needed to provide a final layer of protection against abrasion. For the test, a curved layer of carbon fiber and protective material was created with a radius of 3 in (7.6 cm) to simulate the curved surface of Celeritas. A 105 lb_f (467 N) load was applied to each sample, and the pieces were then dragged across pavement. Every 25 ft (7.6 m), the samples were examined for any hole greater than 0.25 in (6.35 mm) in diameter. When such a hole was found, the sample piece was considered destroyed and its final distance traveled was recorded.

Table 16: Carbon Fiber Penetration Test and Abrasion Test Results

Material	Carbon Fiber Penetration Test	Abrasion Test
Kevlar 5285	Pass	150ft
Kevlar 5120	Pass	200ft
Control-Bare Carbon Fiber	Fail	75ft

Both Kevlar samples effectively stopped carbon fiber pieces from penetrating the protective layer. In the abrasion test, however, the tighter-woven Kevlar 5120 lasted 30% longer than the Kevlar 5285. Kevlar 5120 was chosen for use in the final vehicle instead of Kevlar 5285 because of the lighter weight and increased abrasion resistance.

3.2.5 Skid Testing

Extensive sliding during crashes poses a significant danger to the rider and causes wear to the vehicle. The 2012 Carηot Cycle used automotive trim to lessen skidding. Automotive trim did not fully protect the exterior from wear, was difficult to place, slightly degraded the aerodynamics of the vehicle, and could not be replaced without aesthetic damage.

The team tested rubberized spray paint as a potential replacement to the automotive trim. The 2009 Mark IV had automotive trim applied on its right side and was coated with rubberized spray on its left. A test course with a 200 ft (60.96m) run up and a 50 ft (15.24 m) skid zone was laid out on pavement and the vehicle was crashed three times to each side. There was no noticeable difference between the stopping distances of the two methods. The rubberized paint was not as durable as the automotive trim and would have to be reapplied after 10 to 15 crashes. The durability of the rubberized paint was also examined, as the paint would be required to last through at least one competition before it could be reapplied. The single layer coating of paint wore considerably after three crashes, failing to meet this requirement. Multiple coatings of the rubber could be applied to improve durability, however more time is needed for this process as compared to using automotive trim. The team chose to use automotive trim due to the rubberized spray coating's reduced durability.

To determine where the contact surface would be applied, the vehicle was rolled to each side into a layer of talcum powder. The powder coated the vehicle at contact points and outlined where the automotive trim needed to be applied.

3.2.6 Front Hatch Placement Testing

Once the vehicle geometry and seat position had been finalized, tests were performed to determine the hatch size needed for easy ingress and egress along with the rider's ability to stabilize the vehicle by placing their feet on the ground. The seat height of the 2010 prototype was raised to match Celeritas. Two sheets of plywood were pressed against each side of the rider to constrain the rider to a width of Celeritas, 16 in (40.64 cm), as shown in Figure 20.

Figure 20: Side View of Front Hatch Placement Testing Apparatus

After the rider was appropriately placed and constrained, different elevations of the bottom plane of the hatch were tested by moving the plywood sheets vertically. At each elevation, the weight of the vehicle was modeled by pushing on the riders' shoulders and the riders described their ability to place their feet on the ground while remaining seated. After testing multiple riders of

different heights and leg lengths, the team determined that the sides should not extend more than 7 in (17.78 cm) above the bottom of the seat. The results are shown in Figure 21.

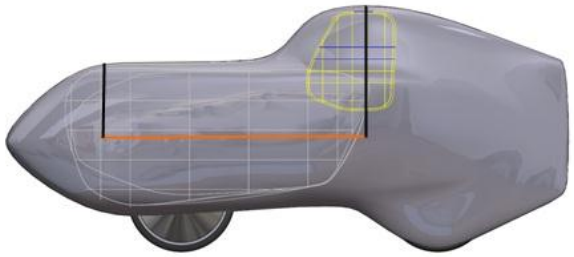

Figure 21: Front Hatch Placement on Celeritas (Determined Elevation in Orange)

3.2.7 Six-Piece Mold Testing

A concern regarding the six-piece mold was whether laying up and curing carbon fiber one half at a time would result in a weak dividing line. To test this, the team made three samples of a single layer of carbon fiber and four samples of two layers of carbon fiber with a Nomex rib in the center approximating the fairing structure.

Half of each of these sample groups were control tests and were cured in one layup. The other samples were cured in two successive layups, each layup curing one half of the sample. In these samples, epoxy was absorbed over the dividing line by 0.25 in (6.35 mm) which would not be detrimental to the vehicle layup.

After curing, all samples were cut to identical sizes and weighed. The double sheet samples were put through a four-point bending test. The flat samples of carbon fiber were too weak to be tested but were still useful for comparing weight and lateral stiffness. The weight and maximum lateral load of each piece tested are shown in Table 17.

Table 17: Discontinuous Layup Testing Results

	Sample	Mass, oz (g)	Max Force, lb_f (N)
Single sheet	1 - control	0.36 (10.3)	Not Tested
	2	0.37 (10.5)	Not Tested
	3	0.37 (10.4)	Not Tested
Double sheet	4 - control	0.86 (24.3)	1590 (7076)
	5 - control	0.83 (23.4)	770 (3426)
	6	0.80 (22.7)	710 (3159)
	7	0.85 (24.2)	1020 (4539)

Sample 4 from the control group endured the maximum force, but sample 5 from the same control batch failed on par with test sample 6. The control and test sample average failure points were similar and could not be distinguished by statistical methods because of the large variation and low sample size. It was also noted that one of the test samples failed away from the middle, suggesting that the dividing line between the two layups was not a significant weak point. It was determined from the results that the two layup methods necessary for the six-piece mold would have no significant impact on the weight or strength of the vehicle.

3.2.8 Gelcoat

The team investigated alternate methods of mold surfacing because the fiberglass layer that was used in previous years was difficult to apply and required large amounts of sanding. The team chose to test a modified gelcoat that was easy to apply as an alternative mold surface. The gelcoat used was a mixture of thick epoxy (cured with 1:1 by volume hardener) and varying amounts of talc powder. The ratio between epoxy and thick hardener in the epoxy solution was kept constant to allow the gelcoat to fully cure while the talc to epoxy solution volumetric ratio was varied between 0.5:1 and 1:1. The gelcoats were applied to 6 x 6 in (15.24 x 15.24 cm) square samples of foam, placed vertically to simulate the sloped surfaces of the mold, allowed to dry, and sanded till smooth.

The trend that emerged in the test results was that as the ratio of talc to epoxy solution was increased from 0.5:1 to 1:1, the samples became thicker and contained fewer bubbles. From the testing, the team decided to use the gelcoat with equal volumes epoxy solution and talc for surfacing the mold.

3.3 Performance Testing

Testing that contributed to the performance of the vehicle is discussed in Section 3.3.1.

3.3.1 Visibility

The rider's visibility from within the vehicle is a crucial component of safety. To test the scope of rider visibility, team members sat in the vehicle and reported the limits of their visibility in each direction. The total visibility was calculated as the average of these reported limits. The results of the testing are displayed graphically in Figure 22. The crosshatching represents the area of the ground that is not visible to the rider.

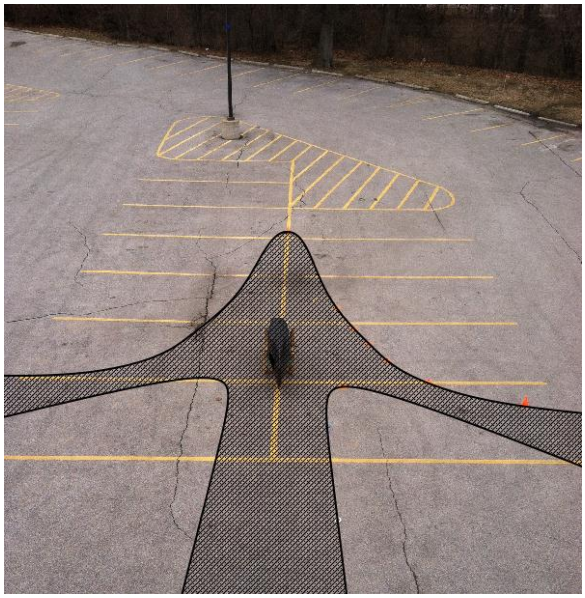

Figure 22: Field of Vision for Celeritas Represented by the Non-Crosshatched Area

The rider has a minimum of 200 degrees of forward visibility and can see the ground 23 ft (7.0 m) in front of the vehicle. Objects any taller than a few inches are visible at much closer ranges to the vehicle, and objects taller than 2 ft (0.61 m) are visible immediately next to the vehicle. Side mirrors mounted on the fairing add 100 degrees of vision to the rear of the vehicle.

4 Safety

Safety is a crucial component of the team as seen in the HoQ where minimizing rider injury is shown as the first and foremost vehicle need, Section 1.5.

4.1 Design for Safety

In the design of Celeritas, safety of the rider and manufacturers was of the utmost concern. Therefore, all components, vehicle systems, and manufacturing methods were evaluated for their safety mechanics prior to implementation.

4.1.1 Roll Bar

A composite roll bar is included in Celeritas to ensure the safety of the rider in a rollover or side impact collision. The roll bar prevents contact between the rider and the road surface and lessens the impact in the event of a crash. The design of the roll bar improves upon that of previous years as described in Section 2.1 and exceeds the competition requirements.

4.1.2 Windshield

The vehicle's windshield is made of polycarbonate, which provides high impact resistance. Because of this, the windshield is very secure and can protect the rider both while riding and during a crash. It gives a total of 300 degrees of visibility, as mentioned in Section 3.3.1, exceeding the competition requirements.

4.1.3 Seatbelt

The seatbelt on Celeritas is a three-point harness as used on the 2012 Carŋot Cycle. It was chosen over a four-point harness to allow for faster ingress and egress times. It is secured in the same fashion as the 2012 Carŋot Cycle, with the top point riveted to a steel plate that is attached to the roll bar. The lower two points are attached to plates embedded in the fairing. Based on previous testing, the belt will hold a total of 1650 lb_f (7335 N) before failing [2], meeting the requirements set forth in the rules. This ensures that the rider will be safe in the event of a crash.

4.1.4 Safety of Manufacturing

In order to ensure the safety of manufacturability of Celeritas, a three-tier system was employed. The first tier was to educate members on the safe use of power tools. Members were not permitted to work alone when using power tools. The second tier required members to use proper personal protective equipment (PPE) when partaking in team activities. Examples of PPE include the use of respirators when sanding carbon and wearing safety glasses at all times. The third tier consisted of a number of decisions to increase safety during construction. An important decision of construction was to use epoxy resin instead of polyester resin, which is cheaper but toxic. In

order to promote further safety, sharp edges on the flanges of the fairing were trimmed off to prevent injury when handling the components.

4.2 Hazard Analysis

Safety of the rider is held paramount when considering any of the components that make up the vehicle. The design also specifically addresses some of the known hazards. To comply with the standard rules of the competition, all riders are required to wear a helmet when in the vehicle. As shown in Section 3.1, the fairing can withstand side impact and rollover situations. In addition to the roll bar, the rider is protected by a roll hoop surrounding their feet. To help protect the shoulders and arms during a crash with the top fairing removed, flanges extend forward from the roll bar.

Kevlar 5120 fabric is used to line the cockpit where the rider sits. In the event that the carbon fiber splinters, the Kevlar acts as a safety net. Sharp edges that have developed during the manufacturing process are either removed or covered by rounded edging.

Uncontrolled skidding after a fall can be more dangerous than the fall itself. To reduce the skidding, rubber automotive trim was placed at contact points on the fairing. The automotive trim also protects the fairing's structural integrity against abrasion.

To help the rider communicate their intentions and make their presence known to other vehicles and pedestrians, standard equipment such as headlights, taillights, brake lights, turn signals, side reflectors, and a loud electronic horn have been installed. The vehicle's low height makes it less visible on the road. To correct this, there is a mounting hole on the back of the vehicle to hold an optional safety flag for increased visibility.

5 Aesthetics

An important factor in a customer's decision to purchase a product is the appearance. For this reason, the team consciously designed to improve the aesthetic appeal of the vehicle both as a newly finished product and throughout its life.

To ensure that the vehicle is attractive, several methods are employed. First, the snap fits, described in Section 1.3, ensure that removable fairing components fit snugly without unattractive gaps. Attention is also given to the paint scheme which serves to mask the unattractive imperfections in the fairing. The interior is also painted to allow the vehicle to appear attractive regardless of fairing configuration. Care is given to internal components to appear clean and professional, and waterproof paint is used to allow for easy cleaning of the vehicle.

When considering the long-term appearance of the vehicle, the team realized that the vehicle will inevitably crash and accumulate scratches and scrapes. The automotive trim used to minimize skidding, as described in Section 4.1, has the added benefit of minimizing contact between the ground and many painted areas of the vehicle. The team has switched to using chopped fiber, which is made by cutting up scrap pieces of carbon fiber and separating individual fibers, then mixing with epoxy to give a fuzzy filler material to fill surface imperfections rather than Bondo.

Chopped fiber appears very similar to laid up carbon fiber, and will degrade more gracefully than Bondo.

6 Conclusion

6.1 Comparison

The team met each design specification listed in Table 1. To verify that the team met its quantitative constraints, they are listed below in Table 18, along with their outcome. The team also met its qualitative constraints: installing mirrors and a rider safety harness, having no exposed carbon, and using a Rose-Hulman school color paint scheme. Celeritas also has an independent and redundant braking system capable of braking from 15 to 0 mph (24.24 to 0 kph) in less than 20 ft (6.10 m).

Table 18: Quantitative Design Constraints and Outcomes

Constraint	Outcome
Total cost of materials and consumables of less than $10,000	The final cost amounted to $2,256.51
The vehicle is less than 8 ft (2.43 m) in length	The final vehicle length is 7 ft 11 in (2.413 m)
Cargo area able to hold a reusable grocery bag of dimensions: 15 x 13 x 8 in (38 x 33 x 20 cm)	Cargo area dimensions: 19 x 15 x 12 in (48 x 38 x 31 cm)
Roll bar that can support 600 lb_f (2.67 kN) top load with elastic deflection less than 2 in (5.1 cm) and 300 lb_f (1.33kN) side load with elastic deflection less than 1.5 in (3.8cm)	Top load of 600 lb_f (2.67 kN) deflects 0.29 in (0.736 cm) and a side load of 300 lb_f (1.33kN) caused a deflection of 0.28 in (0.711 cm)
15 ft (4.57 m) minimum turning radius	13 ft (3.96 m) minimum turning radius

6.2 Evaluations

Celeritas effectively met all of the objectives and design specifications the team set at the beginning of the project. The 25 lb_f (111 N) carbon fiber fairing with integrated rollover protection greatly increases the overall aerodynamics of the vehicle and protects the rider in the event of a crash. By moving the rider to a recumbent position and adding an aerodynamic fairing, the rider can decrease the product of coefficient of drag and cross-sectional area from 6.1 ft^2 (0.56 m^2) on an upright bicycle to 0.27 ft^2 (0.025 m^2) in Celeritas.

Beyond aerodynamic improvements, the fairing protects the rider from the environment. The rider can use Celeritas in adverse weather conditions that would be uncomfortable for the unprotected rider on an upright bicycle. The integrated roll bar and Kevlar protection systems make Celeritas much safer than an upright vehicle in the event of a crash. Celeritas also provides a storage space large enough to accommodate an average grocery bag.

The innovative use of an anti-lock braking system on the Celeritas rear wheel adds additional safety that has not been introduced into the market for an upright or recumbent vehicle.

6.3 Recommendations

Though Celeritas is a capable vehicle that met the team's goals and constraints, there are a few additional features that should be incorporated into the vehicle and processes that should be changed for future vehicle designs. Adding an electric motor and battery pack to Celeritas would greatly increase the marketability and the number of interested parties. An electric motor would allow the rider to maintain pace with higher speed traffic and would help the vehicle up hills. Further iterations of the electric assist system could increase efficiency and versatility by incorporating a regenerative breaking system or another system that allow the rider to recharge the batteries on long trips.

To increase the production scale from a one-off prototype to 10 vehicles per month, the manufacturing process must be adjusted and fine-tuned. This year's mold was not strong enough to be used for more than one vehicle. To increase the durability of the mold, the surface should be reinforced with fiberglass before the application of the gelcoat. The top hatches should be redesigned to allow for access to the rear interior of the fairing during the final layup of the vehicle. The team should also use a vacuum bag that encompasses the entire mold, box, and all excess material hanging over the side of the mold in order to capture any leaks between the sections of the mold.

6.4 Conclusion

The Rose-Hulman Human Powered Vehicle Team set out to create a lightweight, efficient, and agile vehicle that could safely and effectively be used for everyday transportation. The use of advanced composite materials in Celeritas provides an exceptional strength-to-weight ratio that minimizes the material necessary for a full structural fairing. Celeritas is highly efficient when compared to upright bicycles, requiring 22 times less power to overcome air drag at the same speed. Its small frontal profile and streamlined body allow it to travel upwards of 45 mph (73.6 kph), yet it retains low-speed maneuverability with self-stabilization and features like landing gear. Finally, Celeritas protects the rider with an integrated rollover protection system, harness, and Kevlar lining. Its combined efficiency, safety, and utility make it well-suited to capture a market segment in sustainable transportation.

7 Appendices

7.1 Appendix One

Objective

The team developed an anti-lock braking system (ABS) for Celeritas to reduce the number of crashes caused by locking the rear wheel during braking and to increase rider safety. Locking the wheel occurs when the rider applies too much force to the brake which stops the rotation of the wheel. This is common in recumbent vehicles due to the large number of new riders and the different weight distributions between recumbent vehicles and conventional upright bicycles. Less weight on the rear wheel makes it easier to lock up, which causes loss of control of the vehicle. Although ABS is primarily intended for casual riders, even experienced riders will benefit from this system in an emergency when fast, controlled stopping is necessary.

Description

When using a normal disk brake on any bicycle, riders must modulate the brakes to apply a high braking force without locking the rear wheel. This maintains static friction between the wheel and the ground, maximizing braking force and providing control to the rider. Keeping the rear wheel in motion during harsh braking requires skill and concentration, which is difficult to maintain while avoiding a hazard. The ABS developed for Celeritas automates brake modulation.

Due to the weight distribution of the vehicle, the rear wheel will lock before the front wheel. Because the rear wheel will lock first, ABS is only mounted there. Using a cable-actuated brake on the front wheel provides redundancy to mitigate the risks of an ABS failure, such as power loss. This combination of braking systems provides greater safety than either system alone.

The Celeritas ABS is an electromechanical (brake-by-wire) system. The position of the brake lever is measured using a magnet and a Hall Effect sensor. When the brake lever is depressed, the microcontroller instructs a servo to pull a proportional distance on a brake cable to actuate a disk brake.

An optical sensor is positioned near the rear wheel rim, and strips of black paint are equally spaced around the rear wheel rim. The microcontroller uses the time between strips of paint passing the optical sensor to calculate the wheel speed. If the microcontroller detects that the wheel has stopped, the servo reduces the pull on the brake cable until the wheel resumes spinning. Once the wheel has resumed spinning, the microcontroller commands the servo to reapply the brake. This process is continually repeated as long as the brake lever is depressed and the wheel continues to lock, if necessary actuating several times per second. A schematic of the ABS is depicted in Figure 23.

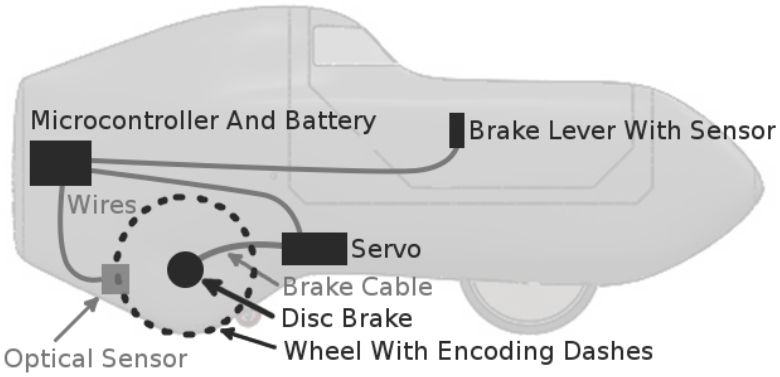

Figure 23: ABS Components for Celeritas

Literature Review

From research, the team discovered that anti-lock braking has a long history. According to the Insurance Institute for Highway Safety, the first use of ABS occurred in airplanes in the 1950s [10]. The use of ABS expanded to automobiles in 1969 with the Ford Thunderbird [10]. ABS for two-wheeled vehicles was introduced in 1988 when BMW debuted the K 100 model motorcycle [11]. Due to ABS's growth in reliability and importance, the U.S. government now requires anti-lock brakes on all passenger vehicles as of the 2012 model year [10].

Many patents mark the advancement of ABS. Filed in 1971, U.S. Patent 3753598 was one of the earliest US ABS patents, describing a "hydraulic antiskid vehicle braking system" [12]. US Patent 5634533 expanded the market in 1994 by patenting an ABS specifically for bicycles and motorcycles [13]. Finally, U.S. Patent 0111342 discussed an electronic ABS system in 2006. It used a wheel speed sensor to judge when to apply braking force from an electric motor through a hydraulic actuator.

ABS is not a novel idea for transportation. However, the basic groundwork of ABS for bicycles is still being laid. According to the team's research, there has been little to no development of ABS specifically for recumbent vehicles. While electronic ABS for bicycles has been patented and is advancing among hobbyists, there are no commercially available products. Furthermore, according to the team's research, all current electronic anti-lock brake systems make use of a hydraulic actuator to apply braking force as opposed to an electronic servo.

The team's ABS is groundbreaking because it is specifically designed for recumbent vehicles. It also is novel because it is an entirely electronic system, utilizing a servo instead of a hydraulic actuator. Even though multiple aspects of the system are covered by existing patents, the team's ABS does introduce an innovative feature set and implementation that is not found in existing literature. Therefore, the system could be patented.

Testing

The Celeritas ABS was developed using a previous year's prototype vehicle. This vehicle had similar geometry to Celeritas with slightly less weight. With ABS disabled, the brake-by-wire system was able to lock the rear wheel, demonstrating that the motor can apply adequate braking force. Testing showed that the vehicle is capable of stopping within the ASME specification

relying on the ABS alone. Furthermore, the ABS prevents the rear wheel from locking when harshly applying the rear brake at a speed of 30 mph (48.6 kph), where this would commonly lock up the rear wheel without it.

Further refinements are being made on the control algorithm, and further testing is planned. Both will be described in the design report update.

Market Analysis

Table 19: Market Analysis for the ABS

Item	Cost
Servo (Futuba S3306)	$40
Microcontroller (ATMega 328P)	$4
Power Electronics	$5
Circuit Board	$10
Optical Sensor	$2
Brake Lever Sensor	$5
Total	***$68***

The total cost of the ABS was under $70. It could be marketed as a $150 add-on feature to Celeritas to improve safety and braking performance, especially for inexperienced riders. Though there are no commercial electronic ABS for upright or recumbent bicycles, there are a few mechanical ABS add-ons for upright bicycles on the market today. King Industries sells a $100 product that produces a strictly mechanical braking frequency by the motion of the wheel, [14] and Budbrake sells a $55 aftermarket brake system that works by applying braking force equally to the front and rear wheels [15]. Winck, Marek, and Ngoo published a paper in the SAE World Congress 2010 showing that a rudimentary pneumatic ABS could greatly benefit emergency braking for bicycles [16].

Recommendations

The ABS has definite improvements which could be made to better the system's benefit to the vehicle. The electrical components could be encased to protect them from water and other debris. By using higher quality components and more efficient design, the overall system sensitivity to rider input could also be increased.

A smaller package and a universal mounting system would allow the ABS to be more functional. This would make the system lighter and easier mount as well as give the team the ability to sell the ABS as a separate component for any bicycle.

The robustness of the system could be improved by utilizing a mechanical backup brake that would override the ABS in the case of a failure. Such a failure could be the effect of power loss or damage to the system. The mechanical backup would improve the safety of the vehicle by allowing the rider to have an auxiliary system.

7.2 Appendix Two

	Per Celeritas	3 year run
Capital Investment		
Machine Subtotal	$130.56	$47,000.00
Tools Subtotal	$3.86	$1,390.00
Total	$134.42	$48,390.00
Tooling		
Layups Subtotal	$316.47	$113,928.00
General Subtotal	$28.35	$10,206.48
Total	$344.82	$124,134.48
Parts and Materials		
Bike Parts Subtotal	$655.04	$235,814.40
Composites Subtotal	$898.13	$323,326.80
Sub Frame Subtotal	$201.01	$72,363.60
Electrical Subtotal	$128.23	$46,162.80
ABS Subtotal	$100.00	$36,000.00
Telemetry Subtotal	$102.00	$36,720.00
Landing Gear Subtotal	$252.29	$90,824.40
Mold Subtotal	$423.13	$152,325.60
Other Subtotal	$50.00	$18,000.00
Total	$1,911.70	$688,210.80
Labor		
Man hours	90.80	32,688.00
Labor Cost	$25.00	$/hr
Total	$2,270.00	$817,200.00
Overhead		
Staff Subtotal	$833.33	$300,000.00
Salary Subtotal	$465.50	$167,580.00
Facilities Subtotal	$154.17	$55,500.00
Utilities Subtotal	$25.00	$9,000.00
Furniture Rental Subtotal	$2.78	$1,000.00
Insurance Subtotal	$69.44	$25,000.00
Total	$1,550.22	$558,080.00
Total Costs:	**$6,211.15**	**$2,236,015.28**

7.3 Appendix Three

Category	Item Purchased	Amount
Tooling		
Layups	Gloves, popsicle sticks, screws	$20.18
	Gloves	$10.69
	Cups, measuring cups, spoons	$7.93
	Peel ply	$147.50
	Breather cloth	$130.00
	Blender	$0.17
	Layups Subtotal:	$316.47
General	Dremel Kit	$1.11
	Replacement Bit for CNC	$4.98
	Sandpaper, Bondo hardener	$19.06
	Sandpaper	$3.21
	General Tooling Subtotal:	$28.35
	Tooling Subtotal:	$344.82
Parts and Materials		
Bike Parts	Tires 2 bikes worth	$132.45
	Shimano Nexus/Alfine 8 speed Shifter	$88.00
	Shifter barrel cable adjusters	$9.99
	Microshift derailleur	$74.00
	9 speed bike chain x4	$27.10
	Tektro calipers	$55.55
	Ultegra derailleur	$84.98
	Chain ring bolts	$29.97
	Cranks	$60.00
	Head tube	$37.00
	Bottom bracket	$26.00
	Fork	$30.00
	Bike Parts Subtotal:	$655.04
Composites	Carbon Fiber (20 yards)	$365.90
	Kevlar	$140.00
	Unidirectional	$119.00
	Epoxy	$200.00
	Polycarbonate	$7.00
	1/4 in Nomex	$36.13
	3/4 in Nomex	$30.10
	Composites Subtotal:	$898.13
Subframe	Steel tubing	$29.68
	Steel bearings	$42.95
	Rectangular tubing	$128.38

	Subframe Subtotal:	$201.01
Electrical	Rechargeable Battery	$48.23
	Wires	$5.00
	White LED's	$20.00
	Red LED's	$15.00
	Bike computer	$40.00
	Electrical Subtotal:	$128.23
ABS	Servo	$50.00
	Potentiometer	$10.00
	Optical Encoder	$20.00
	Microcontroller	$20.00
	ABS Subtotal:	$100.00
Telemetry	2.4 GHz Radios	$40.00
	FTDI Serial to USB	$10.00
	GPS	$40.00
	Misc. Electronics	$12.00
	Telemetry Subtotal:	$102.00
Landing Gear		
	600:1 Gear motor	$24.49
	Teflon bar 3/8” x 3/8” x 5’	$79.92
	Steel tubing	$59.40
	Misc. components	$9.42
	PK27 Geared Motor 27:1	$47.99
	Misc. Electronics	$31.07
	Landing Gear Subtotal:	$252.29
Other	Seat Belt	$44.00
	Thermoform Plastic	$6.00
	Other Subtotal:	$50.00
Molds	Foam	$165.85
	Thick Epoxy, Resin (2 molds)	$123.41
	Caster wheels	$13.86
	Wood	$120.00
	Mold Tooling Subtotal:	$423.13
	Parts and Materials Subtotal:	$1,911.70
	Total:	$2,256.51

Works Cited

[1] Bikes Belong, 2013, "Participation Statistics," Bikes Belong, from www.bikesbelong.org

[2] Rose-Hulman Human Powered Vehicle Team, 2009, "2009 Human Powered Vehicle Team Design Report- West," Terre Haute.

[3] Rose-Hulman Human Powered Vehicle Team, 2010, "2010 Human Powered Vehicle Team Design Report- West,".

[4] Rose-Hulman Human Powered Vehicle Team, 2011, "2011 Human Powered Vehicle Team Design Report- West,".

[5] Rose-Hulman Human Powered Vehicle Team, 2012, "2012 Human Powered Vehicle Team Design Report- West,".

[6] Disley, B.X., 2012, "The effect of Q Factor on gross emchanical efficiency ad muscular activation in cycling ," Scandinavian Journal of Medicing & Science in Sports.

[7] The Weather Channel, 2013, "Average Weather for Big Rapids, MI. and Mountain View, CA.," from www.weather.com

[8] American Society of Mechanical Engineers, 2012, "2013 Human Powered Vehicle Challenge,".

[9] Patterson, W., 1998, *The Chronicles of the Lords of the Chainring*, 5th ed., W.B. Patterson, Santa Maria, CA, p. 109.

[10] Insurance Institute for Highway Safety, 2013, "Q&A: Antilock Brakes," from http://www.iihs.org/research/qanda/antilock.aspx

[11] Bayerische Motoren Werke AG, 1988, "1988 ABS Press Release," from http://www.bmbikes.co.uk/photos/press%20PDF/1988%20ABS%20Press.pdf

[12] Michellone, G., "Hydraulic Antiskid Vehicle Braking System, Having Two Modes of Operation," U.S. Patent Office,.

[13] Zago, M., 1994, "Braking device particularly for bicycles and motorcycles," U.S. Patent Office,.

[14] King Industries, Inc, 2011, "Safe Anti-Locking Braking System," from http://www.kingindustries.ca/SABS.htm

[15] Budbrake, 2012, "Budbrake ABS Modulator," from http://budbrake.com

[16] Wink, R., Marek, K., and Ngoo, C., 2010, "Active Anti-lock Brake System for Low Powered Vehicles Using Cable-Type Brakes," 2010-01-0076, SAE International.

[17] Van Niekerk, J., and Schlesinger, P., 2006, "Bicycle having an antilock brake," U.S. Patent Office,.